SPONGENT: The Design Space of Lightweight Cryptographic Hashing

Andrey Bogdanov, Miroslav Knežević, Gregor Leander, Deniz Toz, Kerem Varıcı, and Ingrid Verbauwhede, *Senior Member*, *IEEE*

Abstract—The design of secure yet efficiently implementable cryptographic algorithms is a fundamental problem of cryptography. Lately, lightweight cryptography—optimizing the algorithms to fit the most constrained environments—has received a great deal of attention, the recent research being mainly focused on building block ciphers. As opposed to that, the design of lightweight hash functions is still far from being well investigated with only few proposals in the public domain. In this paper, we aim to address this gap by exploring the design space of lightweight hash functions based on the sponge construction instantiated with PRESENT-type permutations. The resulting family of hash functions is called SPONGENT. We propose 13 SPONGENT variants—for different levels of collision and (second) preimage resistance as well as for various implementation constraints. For each of them, we provide several ASIC hardware implementations—ranging from the lowest area to the highest throughput. We make efforts to address the fairness of comparison with other designs in the field by providing an exhaustive hardware evaluation on various technologies, including an open core library. We also prove essential differential properties of SPONGENT permutations, give a security analysis in terms of collision and preimage resistance, as well as study in detail dedicated linear distinguishers.

Index Terms—Hash function, lightweight cryptography, low-cost cryptography, low-power design, sponge construction, PRESENT, SPONGENT, RFID

1 Introduction

1.1 Motivation and Related Work

As crucial applications go pervasive, the need for security in RFID and sensor networks is dramatically increasing, which requires secure yet efficiently implementable cryptographic primitives. The most important types of cryptographic algorithms include secret-key ciphers (mainly used to provide data secrecy) and hash functions (multifaceted primitives with the primary usage of data authenticity). In such constrained environments, the area and power consumption of a primitive usually comes to the fore and standard algorithms are often prohibitively expensive to implement.

Once this research problem was identified, the cryptographic community designed a number of tailored lightweight cryptographic algorithms to specifically address this challenge. Stream ciphers (that is, ciphers that process the data in a bitwise manner) like Trivium [10], and block ciphers (i.e., ciphers that operate on blocks of data simultaneously) like KATAN/KTANTAN [11], and PRESENT [5] emerged—to mention only a small selection of the lightweight designs.

- *A. Bogdanov, D. Toz, K. Varıcı, and I. Verbauwhede are with KU Leuven, ESAT/SCD/COSIC, Kasteelpark Arenberg 10, bus 2446, B-3001 Leuven-Heverlee, Belgium and IBBT, Belgium. E-mail: {andrey.bogdanov, deniz.toz, kerem.varici, ingrid.verbauwhede}@esat.kuleuven.be.*
- *M. Knežević is with NXP Semiconductors, Interleuvenlaan 80, 3001 Heverlee, Belgium. E-mail: miroslav.knezevic@nxp.com.*
- *G. Leander is with DTU Mathematics, Technical University of Denmark, Matematiktorvet, Building 303 B, Room 158, 2800 Kgs. Lyngby, Denmark. E-mail: g.leander@mat.dtu.dk.*

Manuscript received 21 Dec. 2011; revised 25 July 2012; accepted 1 Aug. 2012; published online 14 Aug. 2012.
Recommended for acceptance by C. Nita-Rotaru.
For information on obtaining reprints of this article, please send e-mail to: tc@computer.org, and reference IEEECS Log Number TC-2011-12-0968.
Digital Object Identifier no. 10.1109/TC.2012.196.

It was not until recently though that some significant work on lightweight hash functions has been also performed: [6] describes ways of using the PRESENT block cipher in hashing modes of operation and [1] and [14] take the approach of designing a dedicated lightweight hash function based on a sponge construction [9], [2] resulting in two hash functions QUARK and PHOTON.

A *hash function* is a function that maps a bit sequence of arbitrary length to a fixed-length output. As a rule, three security requirements are mentioned for a hash function. First, it should be preimage resistant: Given an output (hash value), it should be hard to find an input (message) that would map to this output. Second, it should be second-preimage resistance: Given a hash value and a corresponding message, it should be difficult to find another message with the same hash value. Finally, it should be collision resistant: It should be infeasible to find two messages with the same hash value.

Among the most prominent security applications targeted by a lightweight hash function are (including the ones requiring preimage security only and collision security only):

- *Lightweight signature schemes*. Elliptic Curve Cryptography (ECC that can be used for both producing digital signatures and public-key encryption) over $\mathbb{F}_{2^{163}}$ is implementable with just 11.904 GE without key storage after synthesis and around 15.000 GE on a chip [16]. For comparison, the smallest published implementation [18] of the NIST-standardized state-of-the-art hash function SHA-256 requires 8.588 GE. The reportedly most compact SHA-3 finalists BLAKE and Grøstl need 13.560 GE [17] and 14.620 GE [24], respectively, to our best knowledge (SHA-3 is the competition launched by NIST to

eventually update the US hash standard). Hence, adding a hashing engine based on SHA-2 to a lightweight ECC implementation would increase its area by at least 50 percent and adding BLAKE or Grøstl would double the area occupation.

- *RFID security protocols* often rely on hash functions. Some of the applications require collision resistance and some of them do not, just needing preimage security. An interesting case is constituted by keyed message authentication codes (MAC) often used in this context. Here, a lightweight hash function can require less area than a lightweight block cipher in a MAC mode at a fixed level of offline and online security. MACs can be also designed using sponge primitives [3].
- *Random number generation* in hardware is used for ephemeral key generation (a temporary key that is used only once and discarded after usage) in public-key schemes, producing random input for cryptographic protocols, and for masking schemes in implementations with protection against side-channel attacks. This frequently needs a preimage-resistant hash function. Using a hash function for pseudorandom number generator (PRNG), given a seed, provides backward security which a block cipher-based PRNG (e.g., in OFB mode) does not: Once the key is leaked, for example, through a side-channel attack, the adversary can compute the previous outputs of the block cipher-based PRNG. Moreover, the postprocessing of a physical random number generator sometimes includes a preimage-resistant hash function.
- *Post-quantum signature schemes* can be built upon a hash function using Merkle trees. There have been several attempts to efficiently implement it [23]. Having a lightweight hash function allows to derive a more compact implementation of the Merkle signature scheme.

However, while for multiple block ciphers, designs have already closely approached the minimum ASIC hardware footprint theoretically attainable, it does not seem the case for some recent lightweight hash functions so far.

1.2 Design Considerations for Lightweight Hashing

The footprint of a hash function is mainly determined by

1. the number of state bits (including the key schedule for block cipher-based designs) as well as
2. the size of functional and control logic used in a round function.

For highly serialized implementations (usually used to attain low area and power), the logic size is normally rather small and the state size dominates the total area requirements of the design. Among the recent hash functions, QUARK, while using novel ideas of reducing the state size to minimize (1), does not appear to provide the smallest possible logic size, which is mainly due to the Boolean functions with many inputs used in its round transform. In contrast to that, SPONGENT keeps the round function very simple that reduces the logic size close to the smallest theoretically possible, thus, minimizing (2) and resulting in a significantly more compact design.

As shown in [6], using a lightweight block cipher in a hashing mode (single block length such as Davies-Meyer or double block length such as Hirose) is not necessarily an optimal choice for reducing the footprint, the major restriction being the doubling of the data path storage requirement due to the feed-forward operation.

At the same time, no feed forward is necessary for the sponge construction, which is the design approach of choice in this work. In a permutation-based sponge construction, let r be the *rate* (the number of bits input or output per one permutation call), c be the *capacity* (internal state bits not used for input or output), and n be the hash length in bits.

1.3 Contributions

This paper proposes the family of sponge-based lightweight hash functions SPONGENT with a smaller footprint than most existing dedicated lightweight hash functions: PRESENT in hashing modes and QUARK. Its area is comparable to that of PHOTON. However, we would like to stress that a fair comparison of sponge-based hash functions in terms of their area requirements is a challenging task. It is not only due to the fact that the area occupation is highly dependent on the implementation, technology, and tools used but also the very parameterization of sponge designs has an immense impact on their hardware performance. By just slightly changing the rate of a sponge-based hash function, one can either make the resulting design smaller and slower or larger and faster. The design of PHOTON opts for a higher rate and a slightly larger area occupation, while SPONGENT chooses for a lower rate and somewhat lower area requirements. With a proper choice of parameters, one can actually turn the situation and make SPONGENT faster though bigger and PHOTON slower but smaller. However, to keep the comparison feasible and representable, we prefer to stick to the original designs in this paper. To address the discrepancies in the hardware design flows, we provide implementation figures for SPONGENT on four different technologies. To make the comparisons fairer, we also provide the hardware figures for SPONGENT, PHOTON, and QUARK based on an open core library.

For some SPONGENT variants, similarly to QUARK and PHOTON, a part of their advantage in terms of low area comes from a reduced level of second-preimage security, while maintaining the standard level collision resistance. The other SPONGENT variants attain the standard preimage, second preimage, and collision security, while having area requirements much lower than those of SHA-1, SHA-2, and SHA-3 finalists. This design subspace has not been specifically addressed by any previous concrete lightweight hash function proposal. Whereas we note that the design ideas of PRESENT in hashing modes, QUARK, and PHOTON might be extended to any set of security parameters.

To explore the design space of lightweight hashing, we propose to instantiate the sponge construction with a PRESENT-type permutation. The resulting construction is called SPONGENT and we refer to its various parameterizations as SPONGENT-$n/c/r$ for different hash sizes n, capacities c, and rates r. SPONGENT is a hermetic sponge, i.e., we do not allow the underlying permutation to have any structural distinguishers. More precisely, for five different hash sizes of $n \in \{88, 128, 160, 224, 256\}$, covering most

security applications in the field, we consider (up to) three types of preimage and second-preimage security levels:

- *Full preimage and second-preimage security*. The standard security requirements for a hash function with an n-bit output size are collision resistance of $2^{n/2}$ as well as preimage and second-preimage resistance of 2^n. For this, in SPONGENT, we set $r = n$ and $c = 2n$ to obtain SPONGENT-88/176/88, SPONGENT-128/256/128, SPONGENT-160/320/160, SPONGENT-224/448/224, and SPONGENT-256/512/256.
- *Reduced second-preimage security*. The design of [1] as well as the papers [2], [3], [9] convincingly demonstrate that a permutation-based sponge construction can allow to almost halve the state size for $n \geq c$ and reasonably small r. In this case, the preimage and second-preimage resistances are reduced to 2^{n-r} and $2^{c/2}$, correspondingly, while the collision resistance remains at the level of $2^{c/2}$. In most embedded scenarios, where a lightweight hash function is likely to be used, the full second-preimage security is not a necessary requirement. For relatively small rate r, the loss of preimage security is limited. So we take this parametrization in the design of the smallest SPONGENT variants with $n \approx c$ for small r and obtain SPONGENT-88/80/8, SPONGENT-128/128/8, SPONGENT-160/160/16, SPONGENT-224/224/16, and SPONGENT-256/256/16. These five SPONGENT-variants were published in a shortened conference version [4] of this paper.
- *Reduced preimage and second-preimage security*. In some applications, the collision security is of concern only and one can abandon the requirement of preimage security to be close to 2^n. In a permutation-based sponge, going for $c = n$ and $r = n/2$ results in the reduction of both the preimage security and second-preimage security to $2^{n/2}$, while maintaining the full collision security of $2^{n/2}$. On the implementation side, this parameterization can yield a favorable ratio between the rate and the permutation size, which reduces the time-area product. We use this approach in the design of SPONGENT-160/160/80, SPONGENT-224/224/112, and SPONGENT-256/256/128.

The group of all SPONGENT variants with the same output size of n bits is referred to as SPONGENT-n. The SPONGENT-88 functions are designed for extremely restricted scenarios and low preimage security requirements. They can be used, for example, in some RFID protocols and for PRNGs. SPONGENT-128 and SPONGENT-160 might be used in highly constrained applications with low and middle requirements for collision security. The latter also provides compatibility to the SHA-1 interfaces. The parameters of SPONGENT-224 and SPONGENT-256 correspond to those of a subset of SHA-2 and SHA-3 to make SPONGENT compatible to the standard interfaces in usual lightweight embedded scenarios.

1.4 Organization of the Paper

The remainder of the paper is organized as follows: Section 2 describes the design of SPONGENT and gives a design rationale. Section 3 presents some results of security analysis, including proven lower bounds on the number of differentially active S-boxes, best differential characteristics found, rebound attacks, and linear attacks. In Section 4, the implementation results are given for a range of tradeoffs. We conclude in Section 5.

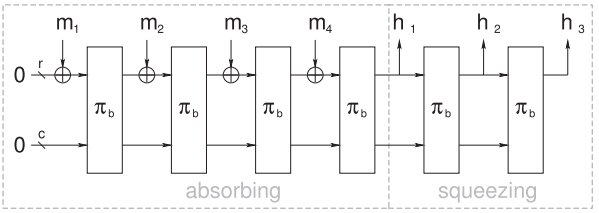

Fig. 1. Sponge construction based on a b-bit permutation π_b with capacity c bits and rate r bits. m_i are r-bit message blocks. h_i are parts of the hash value.

2 The Design of SPONGENT

SPONGENT is a sponge construction based on a wide PRESENT-type permutation. Given a finite number of input bits, it produces an n-bit hash value. A design goal for SPONGENT is to follow the hermetic sponge strategy (no structural distinguishers for the underlying permutation are allowed).

2.1 Permutation-Based Sponge Construction

SPONGENT relies on a sponge construction—a simple iterated design that takes a variable-length input and can produce an output of an arbitrary length based on a permutation π_b operating on a state of a fixed number b of bits. The size of the internal state $b = r + c \geq n$ is called *width*, where r is the *rate* and c the *capacity*.

The sponge construction proceeds in three phases (see also Fig. 1):

- *Initialization phase*. The message is padded by a single bit 1 followed by a necessary number of 0 bits up to a multiple of r bits (e.g., if $r = 8$, then the 1-bit message "0" is transformed to "01000000"). Then, it is cut into blocks of r bits.
- *Absorbing phase*. The r-bit input message blocks are xored into the first r bits of the state, interleaved with applications of the permutation π_b.
- *Squeezing phase*. The first r bits of the state are returned as output, interleaved with applications of the permutation π_b, until n bits are returned.

In SPONGENT, the b-bit 0 is taken as the initial value before the absorbing phase. In all SPONGENT variants, except SPONGENT-88/80/8, the hash size n equals either capacity c or $2c$. The message chunks are xored into the r rightmost bit positions of the state. The same r-bit positions form parts of the hash output.

Let a permutation-based sponge construction have $n \geq c$ and $c/2 > r$, which is fulfilled for the parameter choices of most of the SPONGENT variants. Then, the works [2], [3], [9] imply the preimage security of 2^{n-r} as well as the second-preimage and collision securities of $2^{c/2}$ if this construction is hermetic (that is, if the underlying permutation does not have any structural distinguishers).

TABLE 1
Thirteen SPONGENT Variants

	n (bit)	b (bit)	c (bit)	r (bit)	R number of rounds	security(bit) pre.	2nd pre.	col.
SPONGENT-88/80/8	88	88	80	8	45	80	40	40
SPONGENT-88/176/88	88	264	176	88	135	88	88	44
SPONGENT-128/128/8	128	136	128	8	70	120	64	64
SPONGENT-128/256/128	128	384	256	128	195	128	128	64
SPONGENT-160/160/16	160	176	160	16	90	144	80	80
SPONGENT-160/160/80	160	240	160	80	120	80	80	80
SPONGENT-160/320/160	160	480	320	160	240	160	160	80
SPONGENT-224/224/16	224	240	224	16	120	208	112	112
SPONGENT-224/224/112	224	336	224	112	170	112	112	112
SPONGENT-224/448/224	224	672	448	224	340	224	224	112
SPONGENT-256/256/16	256	272	256	16	140	240	128	128
SPONGENT-256/256/128	256	384	256	128	195	128	128	128
SPONGENT-256/512/256	256	768	512	256	385	256	256	128

The best preimage attack we are aware of in this case has a computational complexity of $2^{n-r} + 2^{c/2}$. Later, this work is extended in [14] and preimage security is defined more generalized form: $min(2^{min(n,\, c+r)}, max(2^{min(n-r,\, c)}, 2^{c/2}))$.

For permutation-based sponge constructions with $n < c$ and $c/2 \leq r$ such as the remaining SPONGENT variants, it follows from the same works that the second-preimage security is 2^n and collision security is $2^{c/2}$. The previous preimage attack also works for this case; hence, we claim that the preimage security is $min(2^n, max(2^{n-r}, 2^{c/2}))$ because $n - r < c$.

2.2 Parameters

We propose 13 variants of SPONGENT with five different hash output lengths at multiple security levels, see Table 1.

2.3 PRESENT-Type Permutation

The permutation $\pi_b : \mathbb{F}_2^b \rightarrow \mathbb{F}_2^b$ is an R-round transform of the input STATE of b bits that can be outlined at a top-level as

for $i = 1$ to R **do**
  $\text{state} \leftarrow \text{pLayer}_b(\text{sBoxLayer}_b(\text{state}) \oplus \text{STATE} \oplus \text{lCounter}_b(i) \oplus \text{rCounter}_b(i))$
end for

where sBoxLayer_b and pLayer_b describe how the STATE evolves. For ease of design, only widths b with $4|b$ are allowed. The number R of rounds depends on block size b and can be found in Section 2.2 (see also Table 1). $\text{lCounter}_b(i)$ is the state of an LFSR dependent on b at time i that yields the round constant in round i and is added to the rightmost bits of STATE. $\text{rCounter}_b(i)$ is the value of $\text{lCounter}_b(i)$ with its bits in reversed order and is added to the leftmost bits of STATE.

The following building blocks are generalizations of the PRESENT structure to larger b-bit widths:

1. *sBoxLayer$_b$*. This denotes the use of a 4-bit to 4-bit S-box $S : \mathbb{F}_2^4 \rightarrow \mathbb{F}_2^4$, which is applied $b/4$ times in parallel. The action of the S-box in hexadecimal notation is given by the following table:

x	0	1	2	3	4	5	6	7	8	9	A	B	C	D	E	F
$S[x]$	E	D	B	0	2	1	4	F	7	A	8	5	9	C	3	6

2. *pLayer$_b$*. This is an extension of the (inverse) PRESENT bit-permutation and moves bit j of STATE to bit position $P_b(j)$, where

$$P_b(j) = \begin{cases} j \cdot b/4 \mod b - 1, & \text{if } j \in \{0, \ldots, b-2\} \\ b - 1, & \text{if } j = b - 1, \end{cases}$$

and can be seen in Fig. 2.

3. *lCounter$_b$*. This is one of the four $\lceil \log_2 R \rceil$-bit LFSRs. The LFSR is clocked once every time its state has been used and its final value is all ones. If ζ is the root of unity in the corresponding binary finite field, the n-bit LFRSs defined by the polynomials given below are used for the SPONGENT variants. Table 2 provides sizes and initial values of all the LFSRs.

LFSR size (bit)	Primitive Polynomial
6	$\zeta^6 + \zeta^5 + 1$
7	$\zeta^7 + \zeta^6 + 1$
8	$\zeta^8 + \zeta^4 + \zeta^3 + \zeta^2 + 1$
9	$\zeta^9 + \zeta^4 + 1$

2.4 Design Rationale

The overall design approach for SPONGENT is to target low area while favoring simplicity.

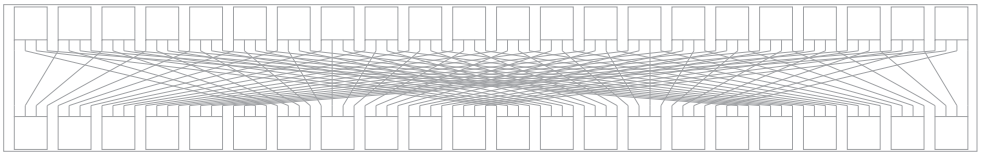

Fig. 2. The bit permutation layer of SPONGENT-88 at the example of pLayer_{88}.

TABLE 2
Initial Values of lCounter$_b$ for all SPONGENT Variants

	LFSR size (bit)	Initial Value (hex)
SPONGENT-88/80/8	6	05
SPONGENT-88/176/88	8	C6
SPONGENT-128/128/8	7	7A
SPONGENT-128/256/128	8	FB
SPONGENT-160/160/16	7	45
SPONGENT-160/160/80	7	01
SPONGENT-160/320/160	8	A7
SPONGENT-224/224/16	7	01
SPONGENT-224/224/112	8	52
SPONGENT-224/448/224	9	105
SPONGENT-256/256/16	8	9E
SPONGENT-256/256/128	8	FB
SPONGENT-256/512/256	9	015

The 4-bit S-box is the major block of functional logic in a serial low-area implementation of SPONGENT. It fulfills the PRESENT design criteria in terms of differential and linear properties [5]. Moreover, any linear approximation over the S-box involving only single bits both in the input and output masks is unbiased. This aims to restrict the linear hull effect discovered in round-reduced PRESENT.

The function of the bit permutation pLayer is to provide good diffusion, by acting together with the S-box, while having a limited impact on the area requirements. This is its main design goal, while a bit permutation may occupy additional space in silicon. The counters lCounter and $\overleftarrow{\text{lCounter}}$ are mainly aimed to prevent sliding properties and make prospective cryptanalysis approaches using properties like invariant subspaces [20] more involving.

The structures of the bit permutation and the S-box in SPONGENT make it possible to prove the following differential property (see Section 3.1 for the proof):

Theorem 1. *Any 5-round differential characteristic of the underlying permutation of* SPONGENT *with* $b \geq 64$ *has a minimum of* 10 *active S-boxes. Moreover, any 6-round differential characteristic of the underlying permutation of* SPONGENT *with* $b \geq 256$ *has a minimum of* 14 *active S-boxes.*

The concept of counting active S-boxes is central to the differential cryptanalysis. The minimum number of active S-boxes relates to the maximum differential characteristic probability of the construction. Since in the hash setting there are no random and independent key values added between the rounds, this relation is not exact (in fact that it is even not exact for most practical keyed block ciphers). However, differentially active S-boxes are still the major technique used to evaluate the security of SPN-based hash functions.

An important property of the SPONGENT S-box is that its maximum differential probability is 2^{-2}. This fact and the assumption of the independency of difference propagation in different rounds yield an upper bound on the differential characteristic probability of 2^{-20} over five rounds and of 2^{-28} over six rounds for $b \geq 256$ which follows from the claims of Theorem 1.

Theorem 1 is used to determine the number R of rounds in permutation π_b: R is chosen in a way that π_b provides at least b active S-boxes. Other types of analysis are performed in the next section.

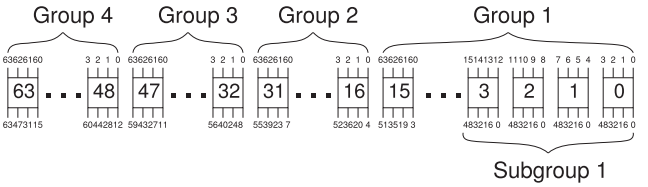

Fig. 3. The grouping and subgrouping of S-boxes for $b = 256$. The input numbers indicate the S-box origin from the previous round and the output numbers indicate the destination S-box in the following round.

3 Security Analysis

In this section, we discuss the security of SPONGENT against known cryptanalytic attacks by applying the most important state-of-the-art methods of cryptanalysis and investigating their complexity.

3.1 Resistance against Differential Cryptanalysis

Here, we analyze the resistance of SPONGENT against differential attacks, where Theorem 1 plays a key role in providing a lower bound on the number of active S-boxes in a differential characteristic. The similarities of the SPONGENT permutations and the basic PRESENT cipher allow to reuse some of the results obtained for PRESENT in [5]. More precisely, the results on the number of differentially active S-boxes over five and six rounds will hold for all respective SPONGENT variants, which is reflected in Theorem 1. The proof of the Theorem 1 is as follows:

Proof (Theorem 1). The statements for SPONGENT variants with $64 \leq b \leq 255$ can directly be proven by applying the same technique used in [5, Appendix III, which can be found on the Computer Society Digital Library at http://doi.ieeecomputersociety.org/10.1109/TC.2012.196]. The proof of the 6-round bounds for SPONGENT variants with $b \geq 256$ in Theorem 1 is based on some extended observations. Here, we will only give the proof for when the width, b, is a multiple of 64 bits, i.e., $b = 64n$. The proof for other b values can also be obtained by making use of the observations given below. Since the proof is specific to each b and, hence, more tedious, we do not present them here.

We obtain n groups and $4n$ subgroups by calling each four consecutive S-boxes as a *subgroup* and each 16 consecutive S-boxes as a *group*. To be more specific, subgroup i is comprised of the S-boxes $[4(i-1)\ldots 4i-1]$ and similarly group j has the subgroups $[4(j-1)\ldots 4j-1]$. (see Fig. 3). By examining the substitution and linear layers, one can make the following observations:

1. The S-box of SPONGENT is such that a difference in single input bit causes a difference in at least two output bits or vice versa.
2. The input bits to an S-box come from four distinct S-boxes of the same subgroup.
3. The input bits to a subgroup of four S-boxes come from 16 distinct S-boxes of the same group.
4. The input bits to a group of 16 S-boxes come from 64 different S-boxes.

5. The four output bits from a particular S-box enter four distinct S-boxes, each of which belongs to a distinct group of S-boxes in the subsequent round.
6. The output bits of S-boxes in distinct groups go to distinct S-boxes in distinct subgroups.
7. The output bits of S-boxes in distinct subgroups go to distinct S-boxes.

For the latter statement (SPONGENT-256), one has to deal with more cases. Consider six consecutive rounds of SPONGENT ranging from i to $i+5$ for $i \in [1, \ldots, 155]$. Let D_j be the number of active S-boxes in round j. If $D_j \geq 3$, for $i \leq j \leq i+5$, then the theorem trivially holds. So let us suppose that one of D_j is equal to one first and to two then. We have the following cases:

Case $D_{i+2} = 1$. By using observation 1, we can deduce that $D_{i+1} + D_{i+3} \geq 3$ and all active S-boxes of round $i+1$ belong to the same subgroup from observation 2. Each of these active S-boxes have only a single-bit difference in their output. So, according to observation 3 we have that $D_i \geq 2D_{i+1}$. Conversely, according to observation 5, all active S-boxes in round $i+3$ belong to distinct groups and have only a single-bit difference in their input. So, according to observation 6, we have that $D_{i+4} \geq 2D_{i+3}$. Moreover, all active S-boxes in round $i+4$ belong to distinct subgroups and have only a single-bit difference in their input. Thus, by using observation 7, we obtain that $D_{i+5} \geq 2D_{i+4}$ and can conclude that $\sum_{j=i}^{i+5} D_j \geq 1 + 3 + 2 \times 3 + 4D_{i+3} \geq 14$.

Case $D_{i+3} = 1$. If $D_{i+2} = 1$, we can refer to the first case. So, suppose that $D_{i+2} \geq 2$. According to the observation 2, all active S-boxes of round $i+2$ belong to the same subgroup and each of these active S-boxes has only a single-bit difference in their output. Thus, according to observation 3, $D_{i+1} \geq 2D_{i+2} \geq 4$. Since all active S-boxes in round $i+1$ belong to distinct S-boxes of the same group and have only a single-bit difference in their input, according to observation 4, we have that $D_i \geq 2D_{i+1}$. On the opposite, D_{i+4} and D_{i+5} can get one and two as a minimum value, respectively. Together this gives $\sum_{j=i}^{i+5} D_j \geq 8 + 4 + 2 + 1 + 1 + 2 \geq 18$.

Case $D_{i+1} = 1$. If $D_{i+2} = 1$, then we can refer to the first case. Thus, suppose that $D_{i+2} \geq 2$. According to observation 5, all active S-boxes in round $i+2$ belong to distinct groups and have only a single-bit difference in their input. Thus, according to observation 6, we have that $D_{i+3} \geq 2D_{i+2}$. Since all active S-boxes in round $i+3$ belong to distinct subgroups and have only a single-bit difference in their input. Therefore, according to observation 7, we have that $D_{i+4} \geq 2D_{i+3}$. To sum up, $\sum_{j=i}^{i+5} D_j \geq 1 + 1 + 2 + 4 + 8 + D_{i+5} \geq 16 + D_{i+5} \geq 17$, because $D_{i+4} > 0$ implies that $D_{i+5} \geq 1$.

Case$D_{i+4} = 1$. If $D_{i+3} = 1$, then we can refer to the second case. So, suppose that $D_{i+3} \geq 2$. According to the observation 2, all active S-boxes of round $i+3$ belong to the same subgroup and each of those active S-boxes has only a single-bit difference in their output. Therefore, according to observation 3, we have that $D_{i+2} \geq D_{i+3}$. Since, all active S-boxes in round $i+2$ belong to distinct S-boxes of the same group and have only a single-bit difference in their input, according to observation 4, we have that $D_{i+1} \geq 2D_{i+2}$. Since $D_{i+1} > 0$, $D_i \geq 1$. Thus, we can conclude that $\sum_{j=i}^{i+5} D_j \geq D_i + 8 + 4 + 2 + 1 + 1 \geq D_i + 16 \geq 17$.

Cases $D_i = 1$ and $D_{i+5} = 1$ are similar to the those for the third and fourth cases.

So far, we have considered all paths including one active S-box in one of the rounds and obtained 14 as the minimum number of active S-boxes. But if there exists a path that has two active S-boxes in each round, then the lower bound would be 12. For this purpose, without loss of generality, assume:

$D_{i+1} = D_{i+2} = D_{i+3} = 2$. The two active S-boxes in $i+2$ are either in the same subgroup or in different subgroups. For the former, from observations 3 and 7, we know that they have single bit of differences coming from two different subgroups of the same group in round $i+1$. From observation 1, these two S-boxes have at least two bits of input difference, hence we obtain $D_i = 4$ by observations 2 and 3. Furthermore, the two S-boxes in round $i+2$ have two bits of output difference by observation 1. Hence, in round $i+3$, the active S-boxes have two bits of input and they are in distinct groups by observation 5. Therefore, it is possible to have $D_{i+4} = 2$ in distinct subgroups. Hence, by using observation 7, we obtain $D_{i+5} = 4$. Thus, we can conclude that $\sum_{j=i}^{i+5} D_j \geq 4 + 2 + 2 + 2 + 2 + 4 \geq 16$.

For the latter, the two active S-boxes in round $i+1$ must have two bits of input and by observation 2 their input bits should be coming from distinct S-boxes in the same subgroup. So, the problem is reduced to the former case with one round of shift, and we can immediately say that $D_i = 2$ and $D_{i+4} = 4$. Hence, by using observation 7, we obtain $D_{i+5} = 4$. Thus, we can conclude that $\sum_{j=i}^{i+5} D_j \geq 2 + 2 + 2 + 2 + 4 + 4 \geq 16$.

Based on these results, we conclude that the longest run with two active S-boxes in each round is four rounds, and the number of active S-boxes cannot be less than 14. □

For all SPONGENT variants, we found that those 5- and 6-round bounds are actually tight. We present the characteristics attaining them in Table 3. Additionally, we perform a branch-and-bound search for longest characteristics with probabilities in the range of 2^{-b}. The results are given in Table 4, most of them based on iterative characteristics.

3.2 Collision Attacks

A natural approach to obtain a collision for a sponge construction is to inject a difference in a message block and then cancel the propagated difference by a difference in the next message block, i.e., $(0 \ldots 0 \| \Delta m_i) \xrightarrow{\pi} (0 \ldots 0 \| \Delta m_{i+1})$. For this purpose, we follow a narrow trail strategy using truncated differential characteristics. We start from a given input difference (some difference restricted to S-boxes that the message block is xored into) and look for all paths that go to a fixed output difference (also located in the bitrate part of the state). Based on our experiments, even by using truncated differential characteristics, the probability of such a path is quite low and it is not possible to attack the full number of rounds.

3.2.1 Rebound Attack

The rebound attack [21], a recent technique for cryptanalysis of hash functions, is applicable to both block cipher-based

TABLE 3
Differential Characteristics with Lowest Numbers of Differentially Active S-Boxes (ASN)

# of	SPONGENT-88/80/8		SPONGENT-128/128/8		SPONGENT-160/160/16		SPONGENT-224/224/16		SPONGENT-160/160/80	
rounds	ASN	Prob	ASN	Prob	ASN	Prob	ASN	Prob	ASN	Prob
5	10	2^{-21}	10	2^{-22}	10	2^{-21}	10	2^{-21}	14	2^{-21}
10	20	2^{-47}	24	2^{-60}	20	2^{-50}	20	2^{-43}	32	2^{-43}
15	30	2^{-74}	40	2^{-101}	30	2^{-79}	30	2^{-66}	52	2^{-66}
# of	SPONGENT-88/176/88		SPONGENT-128/256/128		SPONGENT-160/320/160		SPONGENT-224/224/112		SPONGENT-224/448/224	
rounds	ASN	Prob	ASN	Prob	ASN	Prob	ASN	Prob	ASN	Prob
6	14	2^{-28}	14	2^{-28}	14	2^{-28}	14	2^{-28}	14	2^{-28}
12	41	2^{-96}	37	2^{-72}	39	2^{-93}	36	2^{-88}		
18	64	2^{-158}	52	2^{-119}	65	2^{-157}	66	2^{-174}		
# of	SPONGENT-256/256/16		SPONGENT-256/256/128		SPONGENT-256/512/256					
rounds	ASN	Prob	ASN	Prob	ASN	Prob				
6	14	2^{-28}	14	2^{-28}	14	2^{-28}				
12	32	2^{-73}	50	2^{-123}	34	2^{-84}				
18	52	2^{-128}	68	2^{-169}	54	2^{-128}				

The probabilities are calculated assuming the independency of round computations.

and permutation-based hash constructions. It consists of two main steps: the inbound phase, where the freedom is used to connect the middle rounds by using the match-in-the-middle technique and the outbound phase, where the connected truncated differentials are calculated in both forward and backward directions. It has been mostly used to improve the results on AES-based algorithms (e.g., Grøstl [13]), but it has also been successfully applied to similar permutations (e.g., Keccak [12]).

Compared to the other algorithms the rebound attack has been successfully applied to, the design of SPONGENT imposes some limitations. First of all, because the permutation is bit oriented, and not byte oriented, it might be nontrivial to find the path followed by a given input difference and to determine the number of active S-boxes after several rounds. This is mainly due to the difference propagation that strongly depends on the values of the passive part of the state. Moreover, the probability that two inbound phases match requires more detailed analysis. Below, we attempt to develop rebound attacks on several SPONGENT variants. Rebound analysis applies similarly to the remaining variants.

For SPONGENT-88/80/8, we looked for characteristics that match-in-the-middle with the available degrees of freedom coming from the message bits. For five and more rounds, when the whole state is active in the matching phase, we would not be able to generate enough pairs by using only a difference in the message bits. Since the expected probability of matching the inbound phases is $2^{-b/4}$ (where $b/4$ is the number of S-boxes) and the available degree of freedom is only 2^{2r}, this argument is also valid for SPONGENT-128/128/8, SPONGENT-160/160/16, SPONGENT-224/224/16, and SPONGENT-256/256/16. For other SPONGENT variants, there exist enough degrees of freedom and we decided to explore it with one of the SPONGENT variants.

It is trivial to find one round inbound phase in SPONGENT and then by applying the outbound phase for several rounds, which technically yields a differential characteristic. Since, one-third of the state is xored with the message value for the variants whose rate is different from eight or 16, we have enough flexibility to diffuse the difference through forward and backward direction. But then, merging these differential characteristics seems difficult due to the limited number of pairs generated in the inbound phase.

In our example which is given in Fig. 4, we focused on SPONGENT-128/256/128 and found a five-round trail by following the strategy outlined above. In our attack, we fix

TABLE 4
Longest Differential Characteristics Holding with Probability in the Range of 2^{-b} (under Independency Assumption)

	# rounds	ASN	Prob
SPONGENT-88/80/8	17	34	2^{-88}
SPONGENT-88/176/88	27	103	2^{-268}
SPONGENT-128/128/8	20	56	2^{-137}
SPONGENT-128/256/128	42	146	2^{-385}
SPONGENT-160/160/16	20	66	2^{-179}
SPONGENT-160/160/80	44	88	2^{-242}
SPONGENT-160/320/160	48	192	2^{-480}
SPONGENT-224/224/16	44	88	2^{-242}
SPONGENT-224/224/112	26	133	2^{-343}
SPONGENT-224/448/224	-	-	-
SPONGENT-256/256/16	30	108	2^{-276}
SPONGENT-256/256/128	31	150	2^{-392}
SPONGENT-256/512/256	85	256	2^{-768}

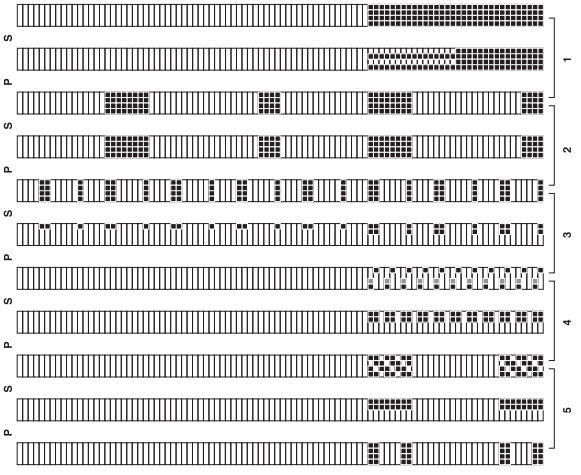

Fig. 4. Differential path for the rebound attack on SPONGENT-128/256/128 (S: $\mathrm{sBoxLayer}_{384}$, P: pLayer_{384}).

TABLE 5
Bounds for Rebound Attack

	2 Inbounds		3 Inbounds	
	rounds /inbound	attacked rounds(%)	rounds /inbound	attacked rounds(%)
SPONGENT-88/80/8	9	40.00	9	60.00
SPONGENT-88/176/88	10	14.81	9	20.00
SPONGENT-128/128/8	15	42.86	14	60.00
SPONGENT-128/256/128	14	14.36	13	20.00
SPONGENT-160/160/16	19	42.22	19	63.33
SPONGENT-160/160/80	19	31.67	19	47.50
SPONGENT-160/320/160	17	14.17	16	20.00
SPONGENT-224/224/16	28	46.67	27	67.50
SPONGENT-224/224/112	23	27.06	23	40.59
SPONGENT-224/448/224	23	13.53	23	20.29
SPONGENT-256/256/16	28	40.00	27	57.86
SPONGENT-256/256/128	28	28.72	27	41.54
SPONGENT-256/512/256	28	14.55	27	21.04

the input and output differences of sBoxLayer in the fourth round. For a half of the differences, we fix the difference to $1_x \rightarrow 3_x$ and for the other half it is possible to fix the difference to either $4_x \rightarrow 3_x$ or $8_x \rightarrow 3_x$, but not both together. Then, we let the differences diffuse for three rounds in the backward direction and for one round in the forward direction. All possible positions of the active bits are shown in black in Fig. 4. Note that in round 5, we impose a restriction on the outputs of the SBoxLayer such that the differences occur only in the bitrate part.

It is possible to generate $4^{11} \cdot 2^{11} = 2^{33}$ pairs in the inbound phase and a pair can satisfy the desired differential trail with a probability of $Pr[B_x \rightarrow \{1_x, 2_x\}]^6 \cdot Pr[D_x \rightarrow \{1_x, 2_x, 3_x\}]^6 \cdot Pr[6_x \rightarrow \{1_x, 2_x\}]^4 = 2^{-26.15}$. Therefore, in total, we expect to have $2^{6.85}$ valid pairs that satisfy the given path.

3.2.2 Bound Considerations for the Rebound Attack

The adversary might try to find a way to attack by using multiple inbounds with a sparse differential. Therefore, to explore the security against multiple inbound phases, we put the adversary into a best-case scenario as follows:

We know that there exists no differential characteristic over five rounds with the number of active S-boxes less than 10 for all SPONGENT variants. We can also deduce lower bounds on the number of active S-boxes for 1, 2, 3, and 4 rounds as 1, 2, 4 and 6, respectively. Then, a bound on the minimum number of active S-boxes, hence the probability of a differential characteristic, for any number of rounds can be approximated by combining these bounds.[1]

The desired bit security level for a sponge construction with respect to collision attacks is $c/2$. From now on, we assume that the complexity of each inbound phase is equal to $c/2$ and at least one active S-box matches between two inbound phases (with probability 2^{-8}). Let n_{in} be the number of inbound phases, then we have to generate $n_{elm} = 2^{8 \cdot (n_{in}-1)/n_{in}}$ elements for each inbound phase. Let p denote the probability of each inbound phase, then p can be at least $2^{-(c/2-\lceil log_2(n_{elm}) \rceil)}$ and we can compute the number of rounds in each inbound phase by using the given bounds above.

1. Note that, Table 3 shows that these bounds might be optimistic.

Under these assumptions, the maximum number of rounds per inbound phase and the percentage of the total number of rounds attacked is given in Table 5.

3.3 Preimage Resistance

Here, we apply a meet-in-the-middle approach to obtain preimages on SPONGENT. The attack has two main steps: precomputation and matching phase Fig. 5. The complexity of the attack is dominated by the precomputation phase.

Since the hash size is n bits, and the data are extracted in r bit chunks, there exists n/r rounds in the squeezing phase. To be able to compute the data backwards in the absorbing phase, we need to know not only h_is but also d_i values to obtain the input value of the permutation π, where h_i denotes the part of the hash value and d_i is the concatenated part to h_i. The algorithm is as follows:

1. *Precomputation*. We know that $\pi^{-1}(h_{i+1}, d_{i+1}) = (h_i, d_i)$ for each i in the squeezing phase. Since h_i (r-bits) is already fixed, the probability of finding such d_i is 2^{-r}. Therefore, we start with $2^{((n/r)-1) \cdot r} = 2^{n-r}$ different $d_{n/r}$ values to have a solution for d_1.
2. *Match-in-the-middle*. Choose k such that $k \cdot r \geq c/2$. Then,
   - Generate $2^{c/2}$ elements in the backward direction by using (h_1, d_1) and possible values for $m_{k+2}, \ldots, m_{2k+1}$ and store them in a table.
   - Generate $2^{c/2}$ elements in the forward direction by using possible values for $m_1, \ldots, m_k$ and compare with list in the previous step to find a match of c bits (corresponding to capacity) in the middle.
   - Obtain m_{k+1} by xor-ing the r bits (corresponding to bitrate) for the matching elements.

In the precomputation part, we obtain the required value d_1 to compute the data backwards in the absorbing phase by 2^{n-r} computations. We need $2^{c/2}$ memory to store the elements generated in the second step and $2^{c/2}$ computations are needed to find a full match. These complexities are exactly given in [25] that extends the bounds given in [9] for $c > n$. We have derived those once again here for completeness. The preimage attack complexities together with the parameter k are given in Table 6.

Note that, if $c \leq n - r$, it is sufficient to try all possible 2^c values to construct the whole state to obtain a preimage; hence, it provides an upper bound for the preimage resistance. If we combine the results, we obtain $max(2^{min(n-r,c)}, 2^{c/2})$ and it can be generalized into the form: $min(2^{min(n,\, c+r)}, max(2^{min(n-r,\, c)}, 2^{c/2}))$. Here, $2^{min(n,\, c+r)}$ computations will be necessary depending on the permutation size when the generic attack, defined above, fails.

3.4 Linear Attacks

The most successful attacks, the attacks that can break the highest number of rounds, for the block cipher PRESENT are those based on linear approximations. In particular, the multidimensional linear attack [7] and the statistical saturation attack [8] claim to break up to 26 rounds. It was shown in [19] that both attacks are closely related. Moreover, the main reason why these attacks are the most successful attacks on PRESENT so far is the existence of

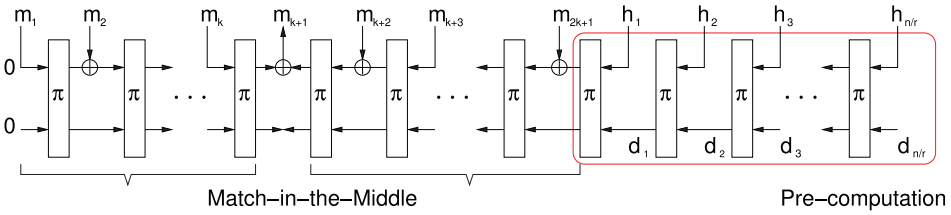

Fig. 5. Meet-in-the-middle attack against sponge construction.

many linear trails with only one active S-box in each round. It is not immediately clear how linear distinguishers on the SPONGENT permutation π_b could be transferred into collision or (second) preimage attacks on the hash function. However, as we claim that SPONGENT is a hermetic sponge construction, the existence of such distinguishers has to be excluded. So the SPONGENT S-box was chosen in a way that allows for at most one trail with this property given a linear approximation.

Unlike for the block cipher PRESENT, where the key determines the actual linear correlation between an input and an output mask, for the permutation π_b we can compute the actual linear trail contribution for all trails with only one active S-box in every round. Each such trail over w rounds has a correlation of $\pm 2^{-2w}$ and for each trail determining the sign is easy. More concretely, one can easily compute a $b \times b$ matrix M_t over the rationals such that the entry at position i, j is the correlation coefficient for round t for the linear trail with input mask e_i and output mask e_j. Here, e_i (resp. e_j) is the unit vector with a single 1 at position i (resp. j). Note that the matrices M_t are sparse and all very similar, the only difference is caused by the round constant, which induces sign changes at a few positions only.

Given those matrices, it is now possible to compute the maximal linear correlation contribution for those 1-bit intermediate masks for all 1-bit input and output masks. For w rounds, we simply compute $M^{(w)} = \prod_{i=1}^{w} M_i$ and the maximal correlation is given by $c_w := \max_{i,j} |M_{ij}^{(w)}|$. We compute this value for all SPONGENT variants. Table 7 summarizes those results. Most importantly, this table shows the maximal number of rounds w, where the trail contributions is still larger than or equal to $2^{-b/2}$. Beyond this number of rounds, it seems unlikely that distinguishers based on linear approximations exist. For most SPONGENT variants, the best linear hull based on single-bit masks has exactly one linear trail.

TABLE 6
Meet-in-the-Middle Attack Results for SPONGENT

	k	Time Complexity $max(2^{n-r}, 2^{c/2})$	Memory Complexity $(2^{c/2})$
SPONGENT-88/80/8	5	2^{80}	2^{40}
SPONGENT-88/176/88	1	2^{88}	2^{88}
SPONGENT-128/128/8	8	2^{120}	2^{64}
SPONGENT-128/256/128	1	2^{128}	2^{128}
SPONGENT-160/160/16	5	2^{144}	2^{80}
SPONGENT-160/160/80	1	2^{80}	2^{80}
SPONGENT-160/320/160	1	2^{160}	2^{160}
SPONGENT-224/224/16	7	2^{208}	2^{112}
SPONGENT-224/224/112	1	2^{112}	2^{112}
SPONGENT-224/448/224	1	2^{224}	2^{224}
SPONGENT-256/256/16	8	2^{240}	2^{128}
SPONGENT-256/256/128	1	2^{128}	2^{128}
SPONGENT-256/512/256	1	2^{256}	2^{256}

TABLE 7
Results of Linear Trail Correlation Based on 1-Bit Masks

	b	max w with $c_w \geq 2^{-b/2}$	R	$\log_2 c_R$
SPONGENT-88/80/8	88	22	45	-90
SPONGENT-88/176/88	264	66	135	-270
SPONGENT-128/128/8	136	34	70	-140
SPONGENT-128/256/128	384	96	195	-388.4
SPONGENT-160/160/16	176	44	90	-180
SPONGENT-160/160/80	240	60	120	-240
SPONGENT-160/320/160	480	122	240	-473.7
SPONGENT-224/224/16	240	60	120	-240
SPONGENT-224/224/112	336	84	170	-340
SPONGENT-224/448/224	673	169	340	-675.3
SPONGENT-256/256/16	272	68	140	-280
SPONGENT-256/256/128	384	96	195	-388.4
SPONGENT-256/512/256	768	192	385	-770

4 Hardware Implementation

In this section, we provide a wide range of hardware figures by evaluating all of the 13 SPONGENT variants in detail. Not only a comprehensive hardware evaluation is of our primary interest, we also further elaborate on the importance of having a unified benchmarking platform for comparing different lightweight designs. We, therefore, provide hardware figures of SPONGENT as well as two state-of-the-art lightweight hash functions (PHOTON and QUARK), all implemented using an open core 45-nm library (NANGATE[2]) [22]. To further stress on the latter issue, we present the performance of SPONGENT using four different CMOS technologies. As it will become apparent, the influence of a library choice on the hardware performance of a single design turns out to be paramount. This phenomenon, in the context of the SHA-3 competition, has been recently discussed in the literature [15].

A fair comparison of hardware performance between different designs has not been sufficiently addressed in the recent publications on lightweight cryptography. It is rather obvious that such comparison is only possible once the highly optimized designs are implemented on the same hardware platform, using the same standard cell library and the same synthesis tool (including the design flow scripts). To eliminate the influence of a specific implementation setup, the same experiment should ideally be

2. We use PDKv1_3_v2009_07 version with the typical case conditions NangateOpenCellLibrary_typical_conditional_ccs.lib.

TABLE 8
Hardware Performance of the SPONGENT Family and Comparison with State-of-the-Art Lightweight Hash Designs Using NANGATE45, an Open Core Library (Postsynthesis Results)

Hash function	Security (bit) Pre.	Coll.	2nd Pre.	Hash (bit)	Cycles	Datapath (bit)	Process (nm)	**Area** (GE)	**Throughput** (kbps)	**Power*** (μW)
SPONGENT-88/80/8	80	40	40	88	990	4	45	869	0.81	16.50
					45	88	45	1237	17.78	38.74
SPONGENT-88/176/88	88	44	88	88	8910	4	45	2264	0.99	33.33
					135	264	45	3633	65.19	140.54
SPONGENT-128/128/8	120	64	64	128	2380	4	45	1257	0.34	21.12
					70	136	45	1831	11.43	53.21
SPONGENT-128/256/128	128	64	128	128	18720	4	45	3183	0.68	44.64
					195	384	45	5715	65.64	232.70
SPONGENT-160/160/16	144	80	80	160	3960	4	45	1572	0.40	24.55
					90	176	45	2406	17.78	73.46
SPONGENT-160/160/80	80	80	80	160	7200	4	45	2066	1.11	30.33
					120	240	45	3612	66.67	143.41
SPONGENT-160/320/160	160	80	160	160	28800	4	45	3931	0.56	54.36
					240	480	45	7163	66.67	282.95
SPONGENT-224/224/16	208	112	112	224	7200	4	45	2070	0.22	31.35
					120	240	45	3220	13.33	96.02
SPONGENT-224/224/112	112	112	112	224	14280	4	45	2827	0.78	41.18
					170	336	45	4611	65.88	182.96
SPONGENT-224/448/224	224	112	224	224	57120	4	45	5430	0.39	72.32
					340	672	45	9751	65.88	429.50
SPONGENT-256/256/16	240	128	128	256	9520	4	45	2323	0.17	34.21
					140	272	45	3639	11.43	109.91
SPONGENT-256/256/128	128	128	128	256	18720	4	45	3183	0.68	44.65
					195	384	45	5713	65.64	232.32
SPONGENT-256/512/256	256	128	256	256	73920	4	45	6163	0.35	81.85
					385	768	45	10778	66.49	447.78
PHOTON-80/20/16 [14]	64	40	40	80	708	4	45	1067	2.82	14.00
					132	20	45	1567	12.15	39.92
PHOTON-128/16/16 [14]	112	64	64	128	996	4	45	1394	1.61	17.20
					156	24	45	2172	10.26	49.62
PHOTON-160/36/36 [14]	124	80	80	160	1332	4	45	1741	2.70	19.37
					180	28	45	2849	20.00	65.78
PHOTON-224/32/32 [14]	192	112	112	224	1716	4	45	2142	1.86	22.63
					204	32	45	3586	15.69	78.82
PHOTON-256/32/32 [14]	224	128	128	256	996	8	45	2675	3.21	51.62
					156	48	45	5335	20.51	248.60
u-QUARK [1]	120	64	64	128	544	1	45	1744	1.47	51.24
					68	8	45	3215	11.76	89.39
d-QUARK [1]	144	80	80	160	704	1	45	2200	2.27	58.59
					88	8	45	3695	18.18	87.74
s-QUARK [1]	192	112	112	224	1024	1	45	3001	3.13	81.55
					64	16	45	6155	50.00	146.01

The nominal frequency of 100 kHz is assumed in all cases and the power consumption is, therefore, estimated accordingly.
**Power figures are based on the post-synthesis results and serve for a qualitative comparison only.*

repeated over many different instances of tools and libraries. Mainly due to the licensing issues and the designer's preference to use a certain software package this, however, becomes a very difficult task in practice.

To partially address this issue, we provide Table 8 where the design of SPONGENT is compared to state-of-the-art lightweight hash functions QUARK and PHOTON, for which the RTL codes are publicly available. The comparison is done using NANGATE45, a publicly available open core library, while the synthesis is carried out using the same script and the same Cadence RTL compiler version 10.10-p104.[3]

What can be seen by observing the obtained data is that for the similar security levels (i.e., SPONGENT-88/80/8 versus PHOTON-80/20/16, SPONGENT-128/128/8 versus u-QUARK versus PHOTON-128/16/16, SPONGENT-160/160/16 versus D-QUARK versus PHOTON-160/36/36, SPONGENT-224/224/16 versus S-QUARK versus PHOTON-224/32/32, and SPONGENT-256/256/16 versus PHOTON-256/32/32), SPONGENT provides a considerably smaller circuit size. On the other hand, mainly due to either a small number of rounds or a higher rate (message block size) both QUARK and PHOTON achieve higher throughput.

Next, we present the obtained hardware figures for all of the SPONGENT variants. For the purpose of extensive hardware evaluation, we use Synopsys Design Compiler version D-2010.03-SP4[4] and target the High-Speed UMC 130-nm CMOS generic process provided by Faraday Technology Corporation (fsc0h_d_tc). The results of all the lightweight implementations are summarized in Fig. 7. It is interesting to observe the wide spectrum of SPONGENT hardware performance, which ranges from the smallest implementation, consuming only 738 GE, until the fastest versions, which achieve more than 66 kbps at 100 kHz.

To provide very compact implementations, we first focus on serialized designs. We explore four different data path

3. Our RTL code and the synthesis scripts are available upon request.

4. KU Leuven owns the Synopsys license.

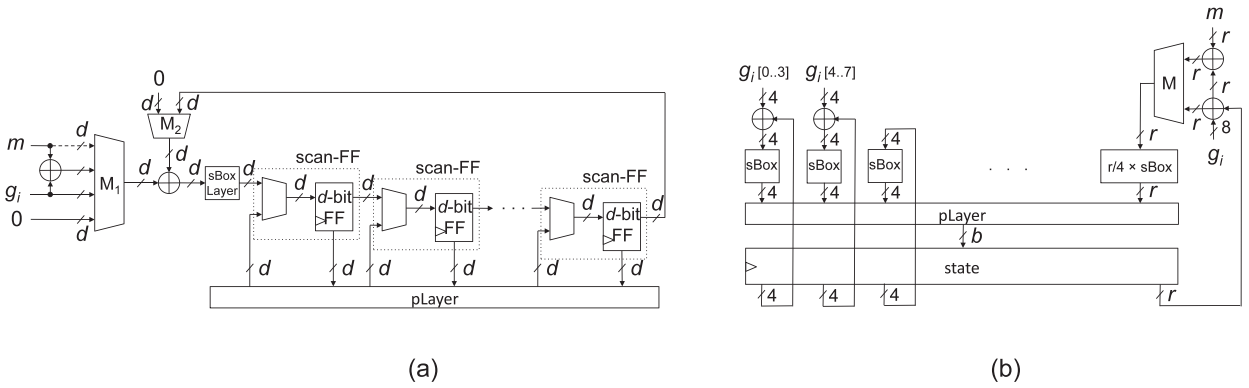

Fig. 6. Hardware architecture representing (a) serial data path, (b) parallel data path of the SPONGENT variants.

sizes (d) for each of the SPONGENT variants and we focus on $d \in \{4, 8, \frac{b}{2}, b\}$. These four implementations are clearly marked in Fig. 7 by the four marker points for each different SPONGENT version. An architecture representing our serialized data path is depicted in Fig. 6a. The control logic consists of a single counter for the cycle count and some extra combinational logic to drive the selection signals of the multiplexers. To further reduce the area we use so-called scan flip-flops, which act as a combination of two input multiplexer and an ordinary D flip-flop.[5] Instead of providing a reset signal to each flip-flop separately, we use two zero inputs at the multiplexers M_1 and M_2 to correctly initialize all the flip-flops. This additionally reduces hardware resources, as the scan flip-flops with a reset input approximately require an additional GE per bit of storage. With g_i we denote the value of $\mathrm{lCounter}_b(i)$ in round i. $\mathrm{lCounter}_b(i)$ is implemented as an LFSR as discussed in Section 2.3. The input of the message block m, denoted with a dashed line, is omitted in some cases, i.e., $d \geq r$. The pLayer module requires no additional logic except some extra wiring.

Using the most serialized implementation, the smallest variant of the SPONGENT family, SPONGENT-88/80/8, can be implemented using only 738 GE. Even the largest member of the family, SPONGENT-256/512/256, consumes only 5.1 kGE, while providing 256 bits of preimage and second-preimage security, and 128 bits of collision resistance. Though some of this advantage is at the expense of a performance reduction, also less serialized (and, thus, faster) implementations result in area requirements significantly lower than 10 kGE. To demonstrate this, we implement all the SPONGENT variants as depicted in Fig. 6b. Every round now requires a single clock cycle, therefore resulting in faster, yet rather compact designs.

Another courtesy of our proposal is the result of five times unrolled design of SPONGENT variants which, all running at the maximum frequency of about 600 MHz, provide a throughput between 360 Mbps and 2 Gbps (depending on the variant) and consume between 5 and 48 kGE.

While it has been well known that the library choice is crucial for the circuit's performance, its impact on a fair comparison between different designs has not been properly addressed in the literature. To highlight its importance, we provide results of SPONGENT implemented using four different standard cell libraries (Table 9). Comparing the

5. Scan flip-flops are typically used to provide scan-chain-based testability of the circuit. Due to the security issues of scan-chain-based testing [26], other methods such as Built-In-Self-Test (BIST) are recommended for testing the cryptographic hardware.

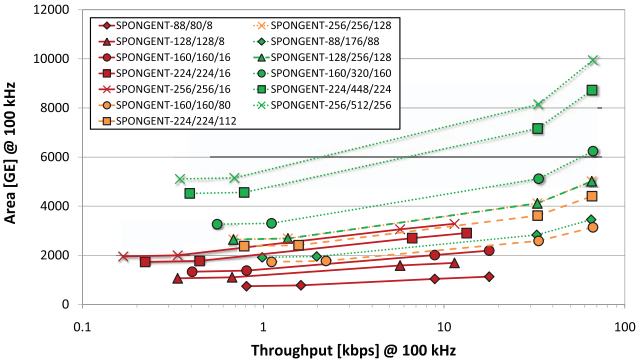

Fig. 7. Area versus throughput tradeoff of the SPONGENT hash family (UMC 130-nm CMOS, postsynthesis results).

TABLE 9
Area of the SPONGENT Family Compared Using Four Different Standard Cell Libraries (Postsynthesis Results)

Hash function	Datapath (bit)	Area (GE) UMC 130 nm	UMC 180 nm	NANGATE 45 nm	NXP 90 nm
SPONGENT-88/80/8	4	738	759	869	521
	88	1127	1232	1237	883
SPONGENT-88/176/88	4	1912	1965	2264	1308
	264	3450	3847	3633	2553
SPONGENT-128/128/8	4	1060	1103	1257	737
	136	1687	1855	1831	1279
SPONGENT-128/256/128	4	2641	2724	3183	1813
	384	5011	5581	5715	4167
SPONGENT-160/160/16	4	1329	1367	1572	918
	176	2190	2241	2406	1752
SPONGENT-160/160/80	4	1730	1769	2066	1192
	240	3139	3434	3612	2650
SPONGENT-160/320/160	4	3264	3340	3931	2232
	480	6237	6949	7163	5262
SPONGENT-224/224/16	4	1728	1768	2070	1192
	240	2903	3203	3220	2334
SPONGENT-224/224/112	4	2371	2422	2827	1621
	336	4406	4900	4611	3197
SPONGENT-224/448/224	4	4519	4625	5430	3069
	672	8726	9696	9751	6932
SPONGENT-256/256/16	4	1950	2012	2323	1340
	272	3281	3721	3639	2612
SPONGENT-256/256/128	4	2641	2724	3183	1813
	384	5011	5581	5713	4213
SPONGENT-256/512/256	4	5110	5232	6163	3471
	768	9944	11054	10778	7426

The nominal frequency of 100 kHz is assumed in all cases.

worst reported performance (i.e., NANGATE45) with the best performance achieved by the advanced NXP90 standard cell library, we discover up to 70 percent difference in area which represents a significant margin (the size is compared using gate equivalences). The main cause of the present variance is a difference in relative cell sizes, which is directly related to the library type. Note that the serial implementation of our designs consists of more than 90 percent of sequential logic. A single scan flip-flop consumes at least 7.67 GE in NANGATE45. The same cell consumes 6.25 and 6.67 GE in UMC130 and UMC180, respectively. The NXP90 library has significantly smaller flip-flops that are the main area consumers in the case of SPONGENT family, and thus provides a considerably better hardware performance.

5 Conclusion

In this work, we have explored the design space of lightweight cryptographic hashing by proposing the family of new hash functions SPONGENT tailored for resource-constrained applications. We consider five hash sizes for SPONGENT—ranging from the ones offering mainly pre-image resistance only to those complying to (a subset of) SHA-2 and SHA-3 parameters. For each parameter set, we instantiate SPONGENT using up to three competing security paradigms (all of them offering full collision security): reduced second-preimage security, reduced preimage and second-preimage security, as well as full preimage and second-preimage security. Each parametrization accounts for its unique implementation properties in terms of ASIC hardware footprint, performance, and time-area product, which are analyzed in the paper. We also perform security analysis in terms of differential properties, linear distinguishers, and rebound attacks.

Acknowledgments

Andrey Bogdanov is a postdoctoral fellow of the Fund for Scientific Research—Flanders (FWO). This work was supported in part by the IAP Programme P6/26 BCRYPT of the Belgian State, by the European Commission under contract numbers ICT-2007-216676 ECRYPT NoE Phase II and ICT-2007-238811 UNIQUE, by KU Leuven-BOF (OT/08/027 and OT/06/40), and by the Research Council KU Leuven: GOA 11/007 TENSE.

References

[1] J.P. Aumasson, L. Henzen, W. Meier, and M. Naya-Plasencia, "Quark: A Lightweight Hash," *Proc. 12th Int'l Workshop Cryptographic Hardware and Embedded Systems (CHES '10),* pp. 1-15, 2010.

[2] G. Bertoni, J. Daemen, M. Peeters, and G. Van Assche, "On the Indifferentiability of the Sponge Construction," *Proc. Theory and Applications Cryptographic Techniques 27th Ann. Int'l Conf. Advances Cryptology (EUROCRYPT '08),* pp. 181-197, 2008.

[3] G. Bertoni, J. Daemen, M. Peeters, and G. Van Assche, "Sponge-Based Pseudo-Random Number Generators," *Proc. 12th Int'l Conf. Cryptographic Hardware and Embedded Systems (CHES '10),* pp. 33-47, 2010.

[4] A. Bogdanov, M. Knezevic, G. Leander, D. Toz, K. Varici, and I. Verbauwhede, "SPONGENT: A Lightweight Hash Function," *Proc. 13th Int'l Conf. Cryptographic Hardware and Embedded Systems (CHES '11),* pp. 312-325, 2011.

[5] A. Bogdanov, L.R. Knudsen, G. Leander, C. Paar, A. Poschmann, M.J.B. Robshaw, Y. Seurin, and C. Vikkelsoe, "PRESENT: An Ultra-Lightweight Block Cipher," *Proc. Ninth Int'l Workshop Cryptographic Hardware and Embedded Systems (CHES '07),* pp. 450-466, 2007.

[6] A. Bogdanov, G. Leander, C. Paar, A. Poschmann, M.J.B. Robshaw, and Y. Seurin, "Hash Functions and RFID Tags: Mind the Gap," *Proc. 10th Int'l Workshop Cryptographic Hardware and Embedded Systems (CHES '08),* pp. 283-299, 2008.

[7] J.Y. Cho, "Linear Cryptanalysis of Reduced-Round PRESENT," *Proc. Int'l Conf. Topics Cryptology (CT-RSA '10),* pp. 302-317, 2010.

[8] B. Collard and F.X. Standaert, "A Statistical Saturation Attack against the Block Cipher PRESENT," *Proc. Int'l Conf. Topics Cryptology (CT-RSA '09),* pp. 195-210, 2009.

[9] G. Bertoni, J. Daemen, M. Peeters, and G. Van Assche, "Sponge Functions," *Proc. Ecrypt Hash Workshop,* May 2007.

[10] C. De Canniè, "Trivium: A Stream Cipher Construction Inspired by Block Cipher Design Principles," *Proc. Ninth Int'l Conf. Information Security (ISC '06),* pp. 171-186, 2006.

[11] C. De Cannière, O. Dunkelman, and M. Knežević, "KATAN and KTANTAN—A Family of Small and Efficient Hardware-Oriented Block Ciphers," *Proc. 11th Int'l Workshop Cryptographic Hardware and Embedded Systems (CHES '09),* pp. 272-288, 2009.

[12] A. Duc, J. Guo, T. Peyrin, and L. Wei, "Unaligned Rebound Attack—Application to Keccak," http://eprint.iacr.org/2011/420, 2011.

[13] P. Gauravaram, L.R. Knudsen, K. Matusiewicz, F. Mendel, C. Rechberger, M. Schläffer, and S.S. Thomsen, "Grøstl—A SHA-3 Candidate," http://www.groestl. info/Groestl.pdf, 2011.

[14] J. Guo, T. Peyrin, and A. Poschmann, "The PHOTON Family of Lightweight Hash Functions," *Proc. 31st Ann. Conference Advances Cryptology (CRYPTO '11)* , pp. 222-239, 2011.

[15] X. Guo and P. Schaumont, "The Technology Dependence of Lightweight Hash Implementation Cost," *Proc. ECRYPT Workshop Lightweight Cryptography,* 2011.

[16] D.M. Hein, J. Wolkerstorfer, and N. Felber, "ECC Is Ready for RFID—A Proof in Silicon," *Proc. Int'l Workshop Selected Areas in Cryptography,* pp. 401-413, 2008.

[17] L. Henzen, J.P. Aumasson, W. Meier, and R.C.W. Phan, "VLSI Characterization of the Cryptographic Hash Function BLAKE," http://131002.net/data/papers/HAMP10.pdf, 2010.

[18] M. Kim, J. Ryou, and S. Jun, "Efficient Hardware Architecture of SHA-256 Algorithm for Trusted Mobile Computing," *Proc. Int'l Conf. Theory and Application of Cryptology and Information Security (Inscrypt '08),* pp. 240-252, 2008.

[19] G. Leander, "On Linear Hulls, Statistical Saturation Attacks, Present and a Cryptanalysis of Puffin," *Proc. 30th Ann. Int'l Conf. Theory and Applications Cryptographic Techniques: Advances in Cryptology,* pp. 303-322, 2011.

[20] G. Leander, M.A. Abdelraheem, H. AlKhzaimi, and E. Zenner, "A Cryptanalysis of PRINTcipher: The Invariant Subspace Attack," *Proc. 31st Ann. Conf. Advances in Cryptology,* pp. 206-221, 2011.

[21] F. Mendel, C. Rechberger, M. Schläffer, and S.S. Thomsen, "The Rebound Attack: Cryptanalysis of Reduced Whirlpool and Grøstl," *Proc. 16th Int'l Workshop Fast Software Encryption (FSE '09),* pp. 260-276, 2009.

[22] NanGate, "The NanGate 45nm Open Cell Library," http://www.nangate.com, 2013.

[23] S. Rohde, T. Eisenbarth, E. Dahmen, J. Buchmann, and C. Paar, "Fast Hash-Based Signatures on Constrained Devices," *Proc. Eighth IFIP WG 8.8/11.2 Int'l Conf. Smart Card Research and Advanced Applications,* pp. 104-117, 2008.

[24] S. Tillich, M. Feldhofer, W. Issovits, T. Kern, H. Kureck, M. Muehlberghuber, G. Neubauer, A. Reiter, A. Koefler, and M. Mayrhofer, "Compact Hardware Implementations of the SHA-3 Candidates ARIRANG, BLAKE, Grøstl, and Skein," http://eprint.iacr.org/2009/349, 2009.

[25] G. Van Assche, "Errata for Keccak Presentation," E-mail sent to the NIST SHA-3 Mailing List on 7 Feb. 2011 on Behalf of the Keccak Team, 2011.

[26] B. Yang, K. Wu, and R. Karri, "Scan Based Side Channel Attack on Dedicated Hardware Implementations of Data Encryption Standard," *Proc. Int'l Test Conf.,* pp. 339-344, 2004.

Andrey Bogdanov received the PhD degree in electrical engineering and computer science from Ruhr University Bochum, Germany, in 2009. He is currently an FWO-supported postdoctoral researcher in the Department of Electrical Engineering, Katholieke Universiteit Leuven, Belgium. In 2011, he was a visiting researcher with Microsoft Research. His interests include cryptanalysis and design of symmetric-key algorithms as well as aspects of provable security and side-channel analysis.

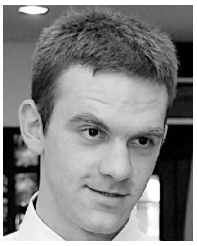

Miroslav Knežević received the MS degree from the University of Belgrade, Serbia, in 2006, and the PhD degree in electrical engineering from the Katholieke Universiteit Leuven, Belgium, in 2011. He is currently a security researcher at NXP Semiconductors. His primary research interests include computer arithmetic and efficient implementations of symmetric-key and public-key cryptographic algorithms.

Gregor Leander received the PhD degree in mathematics from Ruhr University Bochum, Germany, in 2004. He is currently an associate professor at the Technical University of Denmark. His research interests include design and analysis of symmetric cryptography and Boolean functions.

Deniz Toz received the master's degree in cryptography from the Middle East Technical University, Ankara, Turkey, and is currently working toward the PhD degree in the Department of Electrical Engineering, Katholieke Universiteit Leuven, Belgium. Her research interests include symmetric-key components, mainly, analysis and design of symmetric-key primitives, and hash functions.

Kerem Varıcı received the master's degree in cryptography from the Middle East Technical University, Turkey, in 2008. He is currently working toward the PhD degree in the Department of Electrical Engineering, Katholieke Universiteit Leuven, Belgium. His research interests include analysis and the design of the symmetric-key algorithms.

Ingrid Verbauwhede received the electrical engineering and PhD degrees from the Katholieke Universiteit (KU) Leuven, Belgium. She is a professor at the KU Leuven, Belgium. She joined the COSIC Research Group in 2003, and she leads the embedded systems and hardware group of it. In 1998, she was an associate professor at the University of California, Los Angeles (UCLA), where she founded the Embedded Security Research Group. In 2005, she became an adjunct professor at UCLA. She was a postdoctoral visiting researcher and a lecturer at UC Berkeley and was with the TCSI and Atmel in Berkeley, CA. She is a member of the IACR and was an elected member of the Royal Flemish Academy of Belgium for Science and the Arts in 2011. Her primary interest is design, particularly the design methods for secure embedded circuits and systems. She is a senior member of the IEEE.